The Astrophysical Journal, 679: L97–L100, 2008 June 1

THREE-DIMENSIONAL SIMULATION OF MAGNETIZED CLOUD FRAGMENTATION INDUCED BY NONLINEAR FLOWS AND AMBIPOLAR DIFFUSION

Takahiro Kudoh[1] and Shantanu Basu[2]

Received 2008 January 22; accepted 2008 April 23; published 2008 May 2

ABSTRACT

We demonstrate that the formation of collapsing cores in subcritical clouds is accelerated by nonlinear flows, by performing three-dimensional nonideal MHD simulations. An initial random supersonic (and trans-Alfvénic) turbulent-like flow is input into a self-gravitating gas layer that is threaded by a uniform magnetic field (perpendicular to the layer) such that the initial mass-to-flux ratio is subcritical. Magnetic ambipolar diffusion occurs very rapidly initially due to the sharp gradients introduced by the turbulent flow. It subsequently occurs more slowly in the traditional near-quasi-static manner, but in regions of greater mean density than present in the initial state. The overall timescale for runaway growth of the first core(s) is several $\times$ 10^6 yr, even though previous studies have found a timescale of several $\times$ 10^7 yr when starting with linear perturbations and similar physical parameters. Large-scale supersonic flows exist in the cloud and provide an observationally testable distinguishing characteristic from core formation due to linear initial perturbations. However, the nonlinear flows have decayed sufficiently that the relative infall motions onto the first core are subsonic, as in the case of starting from linear initial perturbations. The ion infall motions are very similar to those of neutrals; however, they lag the neutral infall in directions perpendicular to the mean magnetic field direction and lead the neutral infall in the direction parallel to the mean magnetic field.

Subject headings: diffusion — ISM: clouds — ISM: magnetic fields — MHD — turbulence

Online material: mpeg animation

1. INTRODUCTION

In the standard model of low-mass star formation, molecular clouds have an initially subcritical mass-to-flux ratio, and spend a relatively long time ($\sim 10^7$ yr) undergoing quasi-static fragmentation by ambipolar diffusion until cores come to be supercritical. After a core becomes supercritical, it collapses on a dynamical timescale ($\sim 10^6$ yr) to form either one or a small multiple system of stars (e.g., Shu et al. 1987; Mouschovias 1991). Models of nonaxisymmetric fragmentation by this mechanism have been presented recently in several papers (Indebetouw & Zweibel 2000; Basu & Ciolek 2004; Ciolek & Basu 2006; Kudoh et al. 2007, hereafter K07). This scenario is supported by the observed relatively low efficiency of star formation in molecular clouds, i.e., only 1%–5% for clouds as a whole but several times greater within cluster-forming cores (see Lada & Lada 2003). An alternative model is that star formation begins in clouds with supercritical mass-to-flux ratio that have additional support due to turbulence (e.g., Nakano 1998; Hartmann 2001). In this model, star formation occurs relatively rapidly, as turbulence dissipates over a dynamical timescale, and the large-scale magnetic field plays a minor role. The rapid star formation model is supported by the observational results that the age spreads of young stars in nearby molecular clouds are often a few $\times$ 10^6 yr (Elmegreen 2000; Hartmann 2001, 2003), and the low fraction of clouds that are observed to be in a pre-star-formation state.

Recently, Li & Nakamura (2004) and Nakamura & Li (2005) have modeled mildly subcritical clouds and shown that the timescale of cloud fragmentation is reduced by supersonic turbulence. They showed this by performing two-dimensional simulations in the thin-disk approximation. Such a model can explain both relatively rapid star formation and the relatively low star formation efficiency in molecular clouds that is not well explained if star formation starts from a supercritical cloud. In this Letter, we study the three-dimensional extension of the Li & Nakamura (2004) model, by including a self-consistent calculation of the vertical structure and dynamics of the cloud. We confirm that supersonic flows can significantly shorten the timescale of core formation in three-dimensional subcritical clouds, and clarify how the scaling of various physical quantities allows this to occur.

2. NUMERICAL MODEL

We solve the three-dimensional magnetohydrodynamic (MHD) equations including self-gravity and ambipolar diffusion, assuming that neutrals are much more numerous than ions. Instead of solving a detailed energy equation, we assume isothermality for each Lagrangian fluid particle (Kudoh & Basu 2003, 2006). For the neutral-ion collision time and associated quantities, we follow Basu & Mouschovias (1994). The basic equations are summarized in K07.

As an initial condition, we assume hydrostatic equilibrium of a self-gravitating one-dimensional cloud along the z-direction in a Cartesian coordinate system (x, y, z). Although nearly isothermal, a molecular cloud is usually surrounded by warm material, such as neutral hydrogen gas. Hence, we assume that the initial sound speed makes a transition from a low value c_{s0} to a high value c_{sc} at a distance $z = z_c$, with a transition length z_d (see eq. [16] of K07). We take $c_{sc}^2 = 10c_{s0}^2$, $z_c = 2H_0$, and $z_d = 0.1H_0$, where c_{s0} is the initial sound speed at $z = 0$, $H_0 = c_{s0}/(2\pi G\rho_0)^{1/2}$, and ρ_0 is the initial density at $z = 0$. A numerical solution for the initial density distribution shows that it is almost the same as the Spitzer (1942) solution for an equilibrium isothermal layer in the region $0 \le z \le z_c$. We also assume that the initial magnetic field is uniform along the z-direction.

[1] Division of Theoretical Astronomy, National Astronomical Observatory of Japan, Mitaka, Tokyo 181-8588, Japan; kudoh@th.nao.ac.jp.

[2] Department of Physics and Astronomy, University of Western Ontario, London, ON N6A 3K7, Canada; basu@astro.uwo.ca.

A set of fundamental units for this problem are c_{s0}, H_0, and ρ_0. These yield a time unit $t_0 = H_0/c_{s0}$. The initial magnetic field strength (B_0) introduces a dimensionless free parameter

$$\beta_0 \equiv \frac{8\pi p_0}{B_0^2} = \frac{8\pi\rho_0 c_{s0}^2}{B_0^2} = 2\,\frac{c_{s0}^2}{V_{A0}^2}, \quad (1)$$

the ratio of gas to magnetic pressure at $z = 0$. In the above relation, we have also used $V_{A0} \equiv B_0/(4\pi\rho_0)^{1/2}$, the initial Alfvén speed at $z = 0$. In the sheet-like equilibrium cloud with a vertical magnetic field, β_0 is related to the mass-to-flux ratio for Spitzer's self-gravitating layer. The mass-to-flux ratio normalized to the critical value is $\mu_S \equiv 2\pi G^{1/2}\Sigma_S/B_0$, where $\Sigma_S = 2\rho_0 H_0$ is the column density of the Spitzer cloud. Therefore, $\beta_0 = \mu_S^2$. Although the initial cloud we used is not exactly the same as the Spitzer cloud, β_0 is a good indicator of whether or not the magnetic field can prevent gravitational instability. For the model presented in this Letter, we choose $\beta_0 = 0.25$ so that the cloud is slightly subcritical. For this choice, $V_{A0} = 2.8c_{s0}$. Dimensional values of all quantities can be found through a choice of ρ_0 and c_{s0}. For example, for $c_{s0} = 0.2$ km s^{-1} and $n_0 = \rho_0/m_n = 10^4$ cm^{-3}, we get $H_0 = 0.05$ pc, $t_0 = 2.5 \times 10^5$ yr, and $B_0 = 40$ μG if $\beta_0 = 0.25$.

The level of magnetic coupling in the partially ionized gas is characterized by numerical values of the ion number density n_i and neutral-ion collision timescale τ_{ni}. From equations (8) and (9) of K07, and using standard values of parameters in that paper as well as the values of units used above, we find an initial midplane ionization fraction $x_{i,0} = n_{i,0}/n_0 = 9.5 \times 10^{-8}$ and a corresponding neutral-ion collision time $\tau_{ni,0} = 0.11t_0$. The ionization fraction x_i and timescale τ_{ni} at other densities can be found from the initial midplane values given that they both scale $\propto\rho^{-1/2}$ (Elmegreen 1979).

In this equilibrium sheet-like gas layer, we input a nonlinear perturbation to v_x and v_y at each grid point. Independent realizations of v_x and v_y are generated in Fourier space with amplitudes drawn from a Gaussian distribution and consistent with power spectrum $v_k^2 \propto k^{-4}$. Here, $k = (k_x^2 + k_y^2)^{1/2}$ is the total wavenumber. Our adopted power spectrum means that the large scale has more energy than the small scale. This perturbation is consistent with that implemented in Li & Nakamura (2004). The rms value of the initial velocity perturbation in physical space, v_a, is about $3c_{s0}$, so that $v_a \simeq V_{A0}$ as well.

The method of solution and boundary conditions are described by K07 (see also Kudoh et al. 1999; Ogata et al. 2004). The computational region is $|x|,\ |y| \le 8\pi H_0$, and $0 \le z \le 4H_0$, with a number of grid points for each direction (N_x, N_y, N_z) = (64, 64, 40).

3. RESULTS

The top panel of Figure 1 shows the time evolution of the maximum density ρ_{max} at $z = 0$. The simulation is stopped when $\rho_{max} = 30\rho_0$. The solid line shows the result when we input an initially nonlinear supersonic perturbation to the $\beta_0 = 0.25$ model. The dashed line ($\beta_0 = 0.25$) and the dash-dotted line ($\beta_0 = 4$) show the result in the case of the small (linear) initial perturbation that we have applied in K07. This figure shows that the timescale of collapsing core formation for the nonlinear perturbation case is much shorter than that for the linear perturbation case, when β_0 is the same. Even when the initial cloud is subcritical ($\beta_0 = 0.25$), the core formation occurs on almost the same timescale as that of the supercritical ($\beta_0 = 4$) linear perturbation case.[3] The bottom panel of Figure 1 shows the time evolution of the maximum value of density at $z = 0$ (ρ_{max}) and β at the location of maximum density ($\beta_{\rho max}$). At first, $\beta_{\rho max}$ increases rapidly up to ~0.9 due to rapid ambipolar diffusion in the highly compressed regions caused by the initial supersonic perturbation. However, there is enough stored magnetic energy in the compressed region that it rebounds and starts oscillations, with $\beta_{\rho max}$ around 0.7 and increasing gradually. Eventually, $\beta_{\rho max}$ becomes >1 and the dense region collapses to form a core. This figure implies that β is a good indicator to see whether a subregion of the cloud is supercritical or not. The evolution of ρ_{max} confirms that there is an initial compression followed by a rebound to a lower density (still greater than the initial background value) and subsequent oscillations until a runaway collapse starts when continuing ambipolar diffusion has created a region with $\beta > 1$.

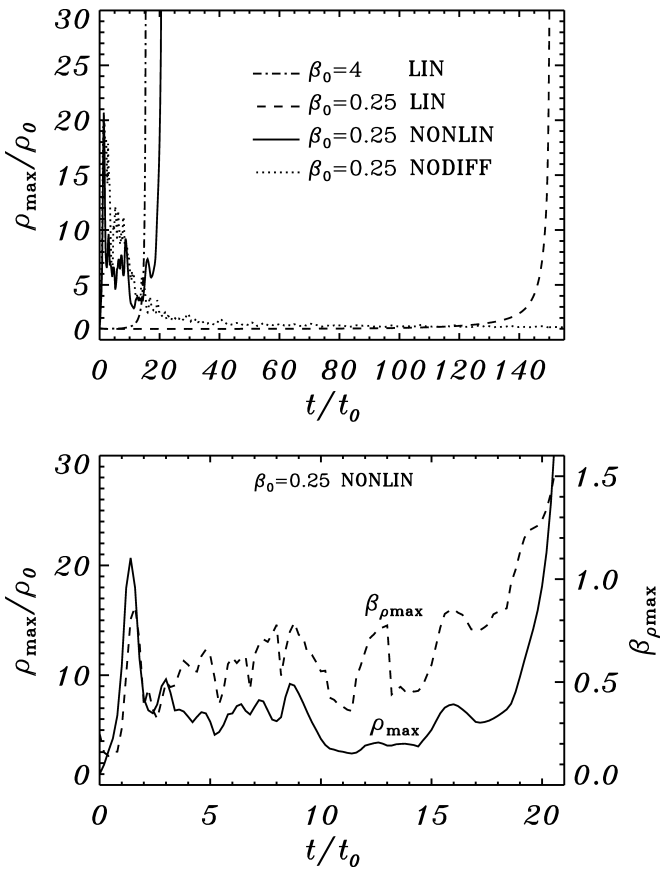

FIG. 1.—*Top*: Time evolution of maximum densities at $z = 0$. The solid line shows the evolution for an initially nonlinear supersonic perturbation and $\beta_0 = 0.25$. The dashed line ($\beta_0 = 0.25$) and the dash-dotted line ($\beta_0 = 4$) show the evolution for models with a linear initial perturbation as calculated by K07. The dotted line shows the evolution for an initially nonlinear supersonic perturbation and $\beta_0 = 0.25$, but without ambipolar diffusion. *Bottom*: Evolution of the maximum density (*solid line*) at $z = 0$ of the simulation box for the model with $\beta_0 = 0.25$ and nonlinear initial perturbation, and evolution of β at the location of maximum density (*dashed line*).

Figure 2 shows an image of the logarithmic density at the last snapshot ($t = 20.5t_0$, when $\rho_{max} = 30\rho_0$) for the nonlinear perturbation case of the subcritical cloud ($\beta_0 = 0.25$). The top panel shows the cross section at $z = 0$, and the bottom panel shows the cross section at $y = -5.9H_0$. The value of y for the

[3] When the initial cloud is supercritical and the perturbation is supersonic, the collapsing core formation happens quickly, at $t \simeq t_0$ from the initial flow. This may be *too* rapid to agree with observations.

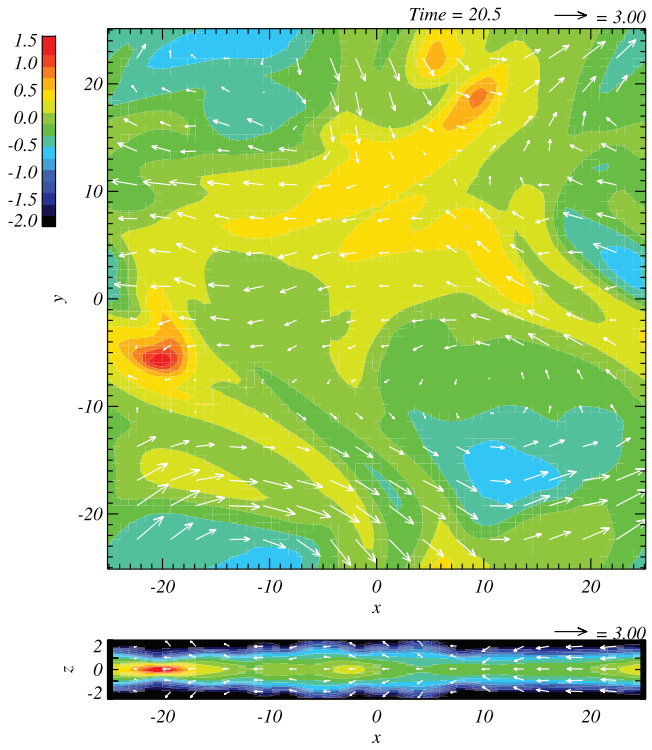

FIG. 2.—Logarithmic density image at $t = 20.5t_0$ for the nonlinear perturbation case of the subcritical cloud ($\beta_0 = 0.25$). The top panel shows the cross section at $z = 0$, and the bottom panel shows the x-z cross section at $y = -5.9H_0$. [*An mpeg animation of the evolution of the density image from* $t = 0$ *to* $t = 20.5t_0$ *is available in the electronic edition of the Journal.*]

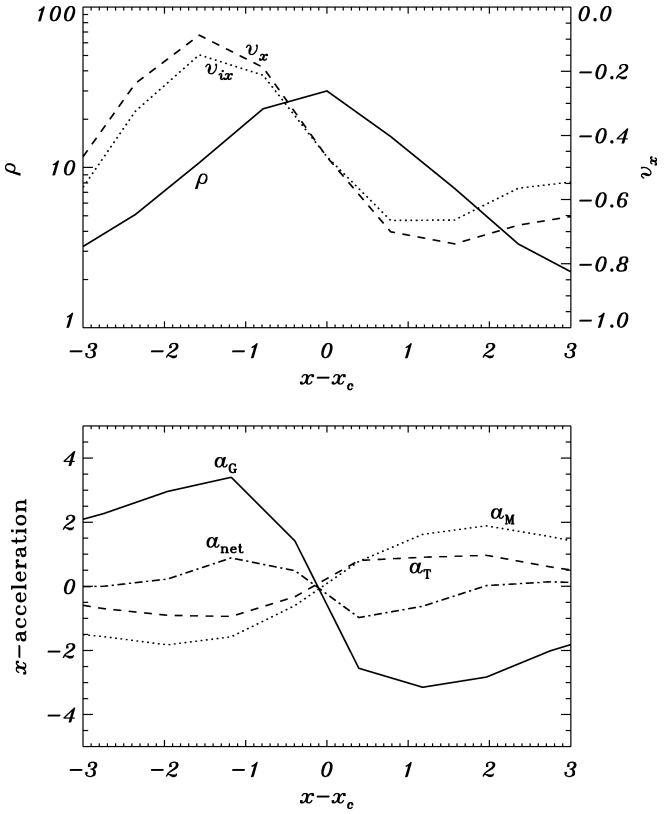

FIG. 3.—*Top*: The density (*solid line*), x-velocity of neutrals (*dashed line*), and x-velocity of ions (*dotted line*) along an x-axis cut at $y = -5.9H_0$, $z = 0$, in the snapshot shown in Fig. 2. The x-positions are measured by offset from $x_c = -20H_0$, which is the maximum density point for the core. *Bottom*: The x-accelerations along the same x-axis as in the top panel. The solid line is the gravitational acceleration (a_G), the dotted line is the magnetic acceleration (a_M), the dashed line is acceleration due to thermal pressure (a_T), and the dash-dotted line is the net acceleration ($a_{\rm net}$). All quantities are normalized by the computational units.

bottom panel is chosen so that the vertical cut passes through the maximum density point. A collapsing core is located in the vicinity of $x = -20H_0$, $y = -5H_0$. The size of the core is similar to that created by linear initial perturbations (see Fig. 2 in K07), although the shape is notably less circular.

The top panel of Figure 3 shows the density and x-velocity of neutrals and ions along an x-axis cut at $y = -5.9H_0$, $z = 0$, taken from the snapshot illustrated in Figure 2. The x-velocities show infall motion toward the center of the core, although the core itself is moving with nonzero negative x-velocity. The relative infall speed to the core is subsonic and about $0.35c_{s0}$. It is comparable to the case of initial linear perturbation (see Fig. 9 in K07). However, there are systematic motions throughout the simulation region that are still supersonic at this time, even though the initial turbulent energy has decayed somewhat. This is qualitatively distinct from the corresponding case with linear perturbations, and should be observationally testable. For the single core that is formed in this simulation, the systematic core motion is about $0.5c_{s0}$ in the x-direction. However, it can be even larger in other realizations. The ion velocity $\boldsymbol{v}_i$ can be related to the neutral velocity $\boldsymbol{v}$ and the magnetic acceleration $\boldsymbol{a}_M$ in the assumed limit of low ion inertia by the relation

$$\boldsymbol{v}_i = \boldsymbol{v} + \boldsymbol{a}_M \tau_{\rm ni}. \tag{2}$$

Figure 3 reveals that the ion infall motions are smaller in magnitude than the neutral motions due to the retarding magnetic acceleration; however, the relative drift in the x-direction between ions and neutrals is typically within $0.05c_{s0}$. In order to see the force balance in the core, we plot the x-accelerations in the bottom panel of Figure 3 along the same x-axis as in the top panel. These values are normalized by the computational units. The inward gravitational acceleration (a_G) dominates around the core. The acceleration from the magnetic force (a_M) and thermal pressure force (a_T) resist the contraction. The net acceleration ($a_{\rm net}$) is working toward the center of the core.

The top panel of Figure 4 shows the density and z-velocities along a z-axis cut at $x = -20H_0$, $y = -5.9H_0$ from the snapshot illustrated in Figure 2. The z-velocities also show infall motion toward the center of the core. The relative neutral infall speed to the core is also subsonic and about $-0.35c_{s0}$. The ion velocity in the vertical direction is almost identical to the neutral velocity but actually very slightly *greater* in magnitude at the peak. The bottom panel of Figure 4 shows the z-accelerations along the same z-axis as in the top panel. In the z-direction, a_G is nearly balanced by a_T, and a_M is almost negligible, *but working in the same direction as gravity*. The net acceleration ($a_{\rm net}$) is also working toward the center of the core. The inward pointing vertical magnetic acceleration associated with an hourglass-type magnetic field morphology explains why the ion velocity in the z-direction is greater in magnitude than the neutral velocity.

4. DISCUSSION AND CONCLUSIONS

Our three-dimensional MHD simulations have shown that the supersonic nonlinear flows significantly reduce the time-

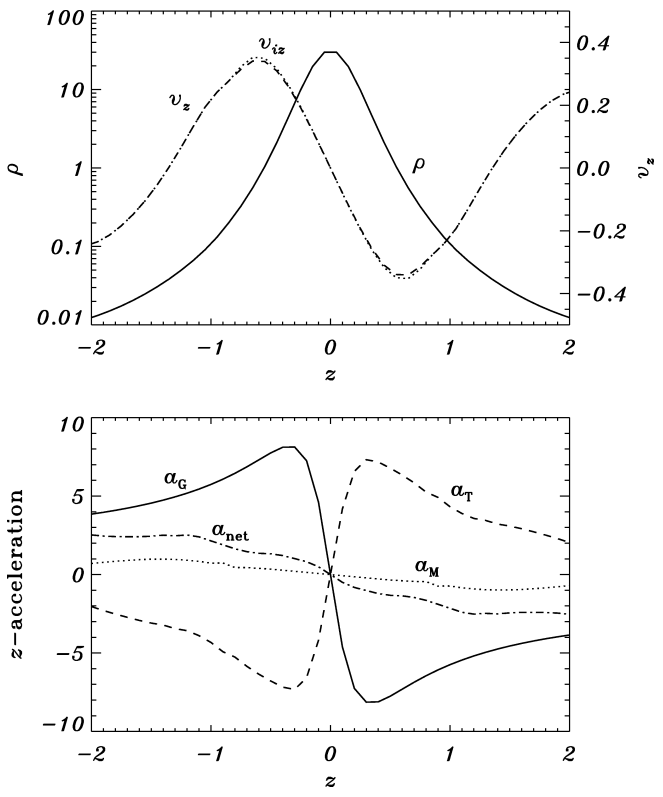

FIG. 4.—*Top*: The density and z-velocity of neutrals and ions along a z-axis cut at $x = -20H_0$, $y = -5.9H_0$, in the snapshot shown in Fig. 2. *Bottom*: The z-accelerations along the same z-axis as in the top panel. The line styles are the same as those in Fig. 3.

scale of collapsing core formation in subcritical clouds. It is of order several $\times$ 10^6 yr for typical parameters, or ~10 times less than found in the linear initial perturbation studies of Basu & Ciolek (2004), Ciolek & Basu (2006), and K07. Our supersonic perturbations are also trans-Alfvénic, in agreement with analysis of observed magnetic field strengths (Basu 2000). It is also in line with the theoretical result of Kudoh & Basu (2003, 2006) that turbulent clouds will settle into a trans-Alfvénic state when global motion/expansion is allowed, even if driven with turbulence that is initially super-Alfvénic.

To see how accelerated ambipolar diffusion can occur, we note that the magnetic induction equation (see, e.g., eq. [3] of K07) and our assumptions of ionization balance can be used to estimate the diffusion time $\tau_d \propto \rho^{3/2}L^2/B^2$, where L is the gradient length scale introduced by the initial turbulent compression and B is the magnetic field strength. Because the compression by the nonlinear flow is nearly one-dimensional, the magnetic field scales roughly as $B \propto L^{-1}$ within the flux freezing approximation. If the compression is rapid enough that vertical hydrostatic equilibrium cannot be established (unlike in previous calculations using the thin-disk approximation), then $\rho \propto L^{-1}$ as well (i.e., one-dimensional contraction without vertical settling), and $\tau_d \propto L^{5/2}$. This means that diffusion can occur quickly (and lead to a rapidly rising value of β) if the turbulent compression creates small values of L. If diffusion is so effective during the first turbulent compression that a dense region becomes magnetically supercritical, then it will evolve directly into collapse. Alternately, the stored magnetic energy of the compressed (and still subcritical) region may lead to a reexpansion of the dense region. The timescale for this, in the flux-freezing limit, is the Alfvén time $\tau_A \propto L\rho^{1/2}/B$, which scales $\propto L^{3/2}$ for the above conditions. Thus, τ_d decreases more rapidly than τ_A, and sufficiently small turbulence-generated values of L may lead to enough magnetic diffusion that collapse occurs before any reexpansion can occur. See Elmegreen (2007) for some similar discussion along these lines. Ultimately, whether or not reexpansion of the first compression can occur depends on the strength of the turbulent compression, mass-to-flux ratio of the initial cloud, and neutral-ion collision time. In a preliminary study of such effects, we found that keeping v_a and β_0 fixed but allowing significantly poorer or stronger neutral-ion coupling yielded differing results. For $\tau_{ni,0} = 0.3t_0$ (poorer coupling), a collapsing core formed due to the first compression, at $t \simeq 1.4t_0$, while for $\tau_{ni,0} = 0.05t_0$ it happened after more oscillations than in our standard model, at $t \simeq 85t_0$. A full parameter study will be required to elucidate.

If reexpansion of the initial compression does occur, as in the standard model presented in this Letter, then there is enough time for the vertical structure to settle back to near-hydrostatic equilibrium, in which case $B \propto \rho^{1/2}$. Since the compressed and reexpanded region executes oscillations about a new mean density, it is convenient to analyze the scalings in terms of the density ρ. The diffusion time now scales as $\tau_d \propto \rho^{-1/2}$. This yields a scaling of τ_d that is the traditionally used one (and is satisfied by design in the thin-disk approximation). However, the diffusion occurs more rapidly than it would in the initial state due to the elevated value of ρ in the compressed but oscillating region (see Fig. 1).

S. B. was supported by a grant from NSERC. Numerical computations were done mainly on the VPP5000 at the National Astronomical Observatory.

REFERENCES

Basu, S. 2000, ApJ, 540, L103
Basu, S., & Ciolek, G. E. 2004, ApJ, 607, L39
Basu, S., & Mouschovias, T. C. 1994, ApJ, 432, 720
Ciolek, G. E., & Basu, S. 2006, ApJ, 652, 442
Elmegreen, B. G. 1979, ApJ, 232, 729
———. 2000, ApJ, 530, 277
———. 2007, ApJ, 668, 1064
Hartmann, L. 2001, AJ, 121, 1030
———. 2003, ApJ, 585, 398
Indebetouw, R., & Zweibel, E. G. 2000, ApJ, 532, 361
Kudoh, T., & Basu. S. 2003, ApJ, 595, 842
———. 2006, ApJ, 642, 270
Kudoh, T., Basu, S., Ogata, Y., & Yabe, T. 2007, MNRAS, 380, 499 (K07)
Kudoh, T., Matsumoto, R., & Shibata, K. 1999, J. Comput. Fluid Dyn., 8, 56
Lada, C. J., & Lada, E. A. 2003, ARA&A, 41, 57
Li, Z.-Y., & Nakamura, F. 2004, ApJ, 609, L83
Mouschovias, T. C. 1991, in Physics of Star Formation and Early Stellar Evolution, ed. C. J. Lada & N. D. Kylafis (Dordrecht: Kluwer), 449
Nakamura, F., & Li, Z.-Y. 2005, ApJ, 631, 411
Nakano, T. 1998, ApJ, 494, 587
Ogata, Y., Yabe, T., Shibata, K., & Kudoh, T. 2004, Int. J. Comput. Methods, 1, 201
Shu, F. H., Adams, F. C., & Lizano, S. 1987, ARA&A, 25, 23
Spitzer, L., Jr. 1942, ApJ, 95, 329